Res Chem Intermed (2018) 44:5301–5327
https://doi.org/10.1007/s11164-018-3424-y

Dinitrophenylhydrazine: β-cyclodextrin inclusion complex as a novel fluorescent chemosensor probe for Ce^{4+}

K. Sivakumar[1] · V. Komathi[1] · M. Murali Krishnan[2]

Received: 29 November 2017 / Accepted: 2 April 2018 / Published online: 13 April 2018

Abstract An inclusion complex of 2,4-dinitrophenyl hydrazine (DNPH) with β-cyclodextrin (β-CD) was prepared and investigated using UV–visible and fluorescence spectral techniques in liquid states, FTIR and NMR techniques in solid state, and molecular docking techniques in virtual states. The binding constants for the formation of 1:1 DNPH: β-CD inclusion complex are estimated by UV–visible and fluorescence spectral techniques. To study the preferred orientation of guest molecules into the host, molecular simulation studies are used. Results of computational studies, semi-empirical analysis and experimental investigations correlate well with each other. The chemosensory power of DNPH: β-CD complex was investigated thoroughly for various metal cations and we found the emission of a complex showed a drastic increase in the intensity for Ce^{4+}. Competition experiments of DNPH: β-CD complex with Ce^{4+} in the presence of other metal ions showed that no significant variation was found in the fluorescence intensity of DNPH:-CD complex upon adding all other cations. The linearity range, LOD and LOQ are determined from the selectivity and sensitivity studies for Ce^{4+}. Our result suggests that the DNPH: β-CD inclusion complex would be promising material for developing a solid state sensory device for sensing Ce^{4+}.

Keywords 2,4-Dinitrophenyl hydrazine · Chemosensor · B-cyclodextrin · Fluorescence enhancement · Cerium ion

✉ K. Sivakumar
chemshiva@gmail.com

[1] Department of Chemistry, Faculty of Science, Sri Chandrasekharendra Saraswathi Viswa Mahavidyalaya University (SCSVMV University), Enathur, Kanchipuram, Tamilnadu 631 561, India

[2] Department of Chemistry, Bannari Amman Institute of Technology, Sathyamangalam 638 401, India

Introduction

The 2,4-dinitrophenylhydrazine (DNPH) is a substituted hydrazine with molecular formula $C_6H_6N_4O_4$. It is synthesized by the action of hydrazine sulfate with 2,4-dinitrochlorobenzene [1]. The intra and intermolecular hydrogen bonds in DNPH have been studied by vibrational spectroscopic analysis [2]. DNPH is an important portion of various biomedical, pharmaceutical products and in toxicology [3, 4]. DNPH can act as colorimetric, fluorescent probes for selective detection of Cu^{2+} ions in nanomolar levels [5]. Dopamine and ascorbic acid can be determined by using a styrene encapsulated DNPH modified GC electrode. DNPH is used to prepare the prulifloxacin [6], determination of pregabalin [7], pyruvic acid in onion pungency [8] and Schiff's base ligand and its metal complexes [9]. Corrosion rates of copper decrease by adding a DNPH and sulphuric acid [10]. The HPLC–DNPH method is used to determine the aldehyde photoproducts from Cu (II)–amino acid complex systems [11]. DNPH has been determining carbonyl modifications of soluble proteins in postmortem samples of substantia nigra, basal ganglia and the prefrontal cortex from neurologically normal subjects, using a DNPH assay [12]. It is used to determine the form of aldehyde in which air containing formaldehyde is sampled by a cartridge containing florisil coated with DNPH [13]. Electrospun polyacrylonitrile nanofiber mats were surface modified by DNPH to yield the metal ion adsorption material, used in wastewater effluents [14].

Cyclodextrins (CD) are a family of cyclic oligosaccharides and possess a cage-like supramolecular structure. In α, β, γ-cyclodextrins, the inner cavities have different diameters which depend upon the glucose unit's number. CDs form inclusion complexes with a variety of organic molecules. The hydrophobic central cavity of CDs preferentially accommodates hydrophobic guest molecules and forms inclusion complexes [15–18]. Cyclodextrins are able to form inclusion complexes with hydrophobic molecules and give a unique nature for the complex [19]. Cyclodextrins or their derivatives make them suitable for applications in analytical chemistry, pharmaceutical fields [17, 20–24], food [25–28], agriculture [29–31], textiles [32], antibacterial fields, and toilet articles. For removing environmental impurities, host guest systems have been utilized.

Cerium is a rare earth element abundant as monazite and bastnasite. Cerium (IV) is industrially important and is used in nuclear reactors, metallurgy industries, microwave devices, lasers, agriculture, glass industries and in many other commercial applications [33–35]. Cerium nitrate with silver sulfadiazine is used for producing antiseptic agents [36]. Modern developments in nanotechnology accumulates cerium in the environment due to the extensive use of CeO_2 (ceria) in catalysis [37, 38], polishing [39], energy [40], electronics [41], pigmentation [42], hydrogen production [43], fuel additive processes [44], automobiles [45], inflammation [46, 47], apoptosis [48], protein signaling [49] and biomedicals [50]. Cerium is used in electronic gadgets such as televisions, glasses and lamps [51, 52]. It is highly possible that cerium can be concentrated in the atmospheric air due to the emission from these gadgets leading to the penetration of cerium in the human body.

Continuous exposure of cerium causes thrombotic effects in the lung [53] and liver inflammation [54].

Hence, establishing a systematic analysis mechanism for the estimation of Ce^{4+} ions are necessary. Spectrophotometric estimation of Ce^{4+} using p-nitro aniline [55], azocalixarene [56], malachite green iodide [57], benzoic hydrazone [58],and spectrofluorometric estimation of Ce^{4+} using 2, 6-diaminotoluene [59], ascorbic acid [60], and potentiometric estimation of Ce^{4+} [61] are reported in the literature.

During the complexation investigation, significant increase in the fluorescence intensity of DNPH:β-CD and further enhancement for the addition of Ce^{4+} are observed. Hence, based on the observation of fluorescence enhancement of DNPH: β-CD + Ce^{4+} a method for the determination of Ce^{4+} using DNPH: β-CD complex as a fluorescent chemosensor has been developed. The complexation analysis and estimation of binding constants has been carried out using absorption and fluorescence spectral analysis. The host–guest complex formation was confirmed by FTIR, NMR and semi-empirical calculations. The chemosensing behavior of DNPH: β-CD complex was carried out using fluorescence spectroscopy. The results suggest that the DNPH: β-CD host–guest inclusion complex can be used as a chemosensor for detecting Ce^{4+} in liquids.

Materials and methods

Instruments and reagents

DNPH and β-CD were obtained from HiMedia laboratories (Mumbai) and used without further purification. Triply distilled water was used to prepare all solutions and spectrograde solvents were used. For complexation studies the concentration of β-CD was varied from 0 to 0.018 M. The UV spectra were recorded with an analytic Jena, Germany, spectrophotometer. Fluorescence spectra of each solution were recorded between 380 and 800 nm excited at 366 nm with a Perkin Elmer LS-45 fluorescence spectrophotometer. The solid inclusion complex was prepared by the co-precipitation method. The IR spectra of all samples were recorded using an Alpha-T FTIR spectrometer (Bruker optics) equipped with an OPUS version 6.5 by the KBr pellet method. ^{1}H NMR and ^{13}C NMR were taken by a BRUKER NMR instrument in $CDCl_3$ at 300 K.

Molecular docking study

By molecular docking studies and a Patch Dock server, the most probable structure of the DNPH: β-CD inclusion complex was determined [62]. The 3-D structural data of β-CD and DNPH was obtained from crystallographic databases. The Patch Dock server is an online source for the docking of the guest molecule DNPH into the host molecule (β-CD) cavity by submitting the 3-D coordinate data of DNPH and β-CD molecules. Docking was performed with complex type configuration settings. The Patch Dock server follows a geometry-based molecular docking algorithm to find the docking transformations with good molecular shape

complementarity. The Patch Dock algorithm separates the Connolly dot surface representation [63, 64] of the molecules into concave, convex and flat patches. The patches are used for a geometric fit evaluation and an atomic desolvation energy scoring [65] function. Root mean square deviation (RMSD) clustering is applied to the docked solutions to select the non-redundant results and to discard redundant docking structures.

Semi-empirical quantum mechanical calculations

The ground state of the DNPH molecule was optimized using the Argus Lab program by the AM1 and PM6 method. The Mol Soft Mol Browser tool was used to visualize the 3-D structural data.

Orientation preference analysis

With the objective of judging the preference of the guest molecule (DNPH) in the host molecule (β-CD) for forming an inclusion complex, detailed investigation on the orientation preference analysis of guest into host has been carried out and the energy differences in the inclusion process are calculated using the GAUSSIAN 03 [66] software package using the AM1 and PM6 method.

For orientation preference analysis, the 3-D structures of guest (DNPH) and host (β-CD) molecules are optimized without any symmetry constraints. Figure 7 represents two different orientations considered for the inclusion of DNPH through the 2° (wide) rim of the β-CD cavity.

Orientation 1: orientation of the hydrazine group of DNPH towards the 2° rim of β-CD (Fig. 7a).

Orientation 2: orientation of the nitro group containing DNPH towards the 2° rim of β-CD (Fig. 7b).

For the models "*Orientation* 1" and "*Orientation* 2" the single point energy is computed using the AM1 and PM6 method by the GAUSSIAN 03 software package. First, the DNPH molecule is placed at a z-coordinate of 6 Å and simulated via the β-CD cavity along the z-axis to − 6 Å with a little-by-little increment of 1 Å. From ten complex models of DNPH:β-CD obtained, the very low energy most stable complex models of "*Orientation* 1" and "*Orientation* 2" are identified based on an energy versus distance comparison. Further, the most stable models of "*Orientation* 1" and "*Orientation* 2" are optimized to minimize the energy.

General procedures of spectra detection

By Job's method, also known as the continuous variation method, the 1:1 stoichiometry of an inclusion complex was confirmed [67]. For this, stock solutions are prepared with equimolecular concentrations of β-CD and DNPH. To investigate the influence of metal ions on the fluorescence spectra of DNPH: β-CD complex, a stock solution of β-CD (12×10^{-3} M) and a stock solution of metal ions (10^{-4} M) were prepared by dissolving the appropriate amount of substance in double distilled water. The concentration of DNPH is 10^{-3} M and prepared in methanol. For

recording fluorescence spectra, the dilute solutions are prepared by mixing an appropriate amount of stock solutions for the β-CD + DNPH + metal ion. Fluorescence spectra of each solution were recorded between 380 nm to 800 nm excited at 366 nm.

Result and discussion

Interaction of DNPH with β-CD in liquid state

UV spectral analysis

Table 1 and Fig. 1a show the absorption spectral data of DNPH on varying concentrations of β-CD from 0 to 18 × 10^{-3} M. There is an enhancement in the absorbance for increasing the concentration β-CD that shows the increasing solubility and formation of an inclusion complex between β-CD and DNPH. For the inclusion complex between host and guest (DNPH: β-CD), the equilibrium exists.

$$\text{DNPH} + \beta\text{-CD} \overset{K}{\leftrightarrows} \text{DNPH}\ldots\beta\text{-CD}$$

The Benesi–Hildebrand [68] relation is used for the estimation of binding constant '*K*' by assuming the formation of a 1:1 host–guest complex,

Table 1 Absorption and fluorescence maxima (nm) of DNPH (1 × 10^{-3} M) at different concentrations of β-CD water

S. no.	Concentration of β-cyclodextrin (M)	UV			Fluorescence	
		λ_{max} (nm)	Abs	log e	λ_{Flu} (nm)	Flu. intensity
1	Without β-CD	366	0.133	2.12	425	507.16
2	0.002	366	0.150	2.06	425	524.35
3	0.004	366	0.148	2.17	425	531.52
4	0.006	366	0.151	2.18	425	543.78
5	0.008	366	0.155	2.19	425	563.16
6	0.010	366	0.158	2.20	425	588.19
7	0.012	366	0.148	2.17	425	659.10
8	0.014	366	0.174	2.24	425	702.08
9	0.016	366	0.158	2.20	425	725.02
10	0.018	366	0.155	2.19	425	1010.02
Binding constant ($M^{1)}$			500		588	
ΔG (kJ mol^{-1})			− 15.88		− 15.48	

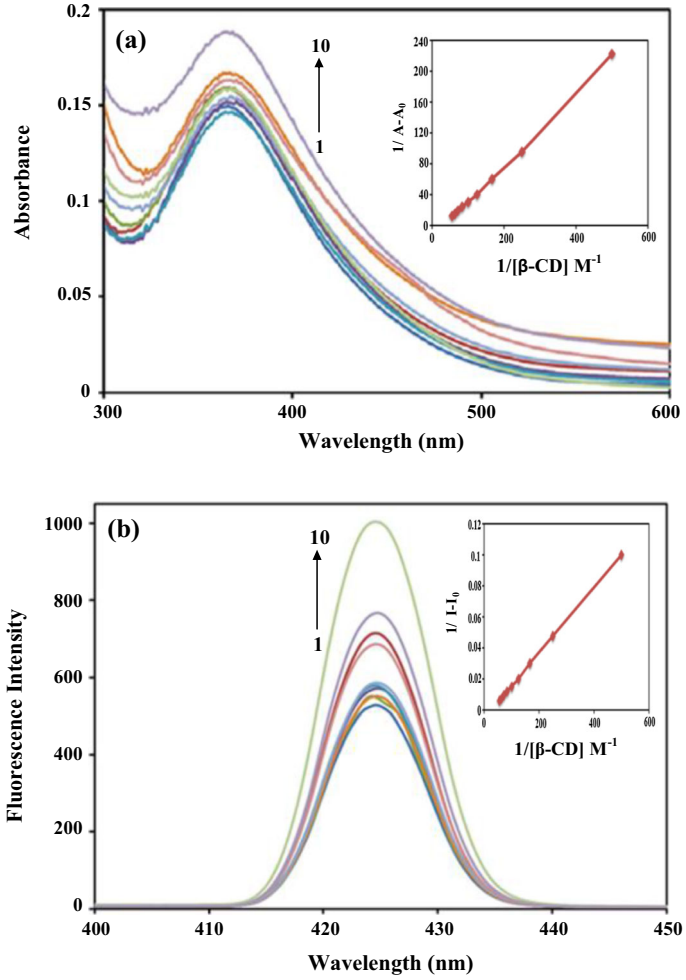

Fig. 1 **a** Absorption and **b** fluorescence spectra of DNPH (10^{-3} M) in pH $\sim$ 7 solution with different β-CD concentrations: (1) 0.0 M (2) 0.002 M (3) 0.004 M (4) 0.006 M (5) 0.008 M (6) 0.01 M (7) 0.012 M (8) 0.014 M (9) 0.016 M (10) 0.018 M insets: Benesi-Hildebrand plot

$$\frac{1}{A - A_0} = \frac{1}{\Delta\varepsilon} + \frac{1}{K[\text{DNPH}]_0 \, \Delta\varepsilon \, [\beta\text{-CD}]_0}.$$

where A and A_0 are the difference between the absorbance of DNPH in the presence and absence of β-CD, $\Delta\varepsilon$ is the difference between the molar absorption coefficient of DNPH and the inclusion complex, $[\text{DNPH}]_0$ and $[\beta\text{-CD}]_0$ are the initial concentrations of DNPH and β-CD, respectively. The plot of $1/A - A_0$ versus 1/[β-CD] for DNPH, shows a good linear correlation [inset of Fig. 1], and confirms the formation of 1:1 inclusion complex. From the intercept and slope values of the plot, the binding constant '*K*' evaluated as 500 M^{-1}.

Fluorescence analysis

In the emission spectral data of DNPH [Fig. 1b; Table 1] the fluorescence intensity increases for the variation of β-CD concentration from 0 to 18 × 10^{-3} M. These results indicate that DNPH is entrapped into the β-CD cavity to form DNPH: β-CD inclusion complex. The binding constant for the formation of the complex has been determined by analyzing the changes in the intensity of emission maxima with the β-CD concentration using the Benesi-Hildebrand [68] relation assuming the formation of a 1:1 host–guest complex.

$$\frac{1}{I - I_0} = \frac{1}{I' - I_0} + \frac{1}{K\,[I' - I_0]\,[\beta\text{-CD}]_0}$$

where $[\beta\text{-CD}]_0$ represents the initial concentration of β-CD, "I_0" and "I" are the fluorescence intensities in the absence and presence β-CD, respectively, and I' is the limiting intensity of florescence. The 'K' value was estimated from the slope and intercept of the Benesi–Hildebrand plot (inset of Fig. 2) which shows a good linear

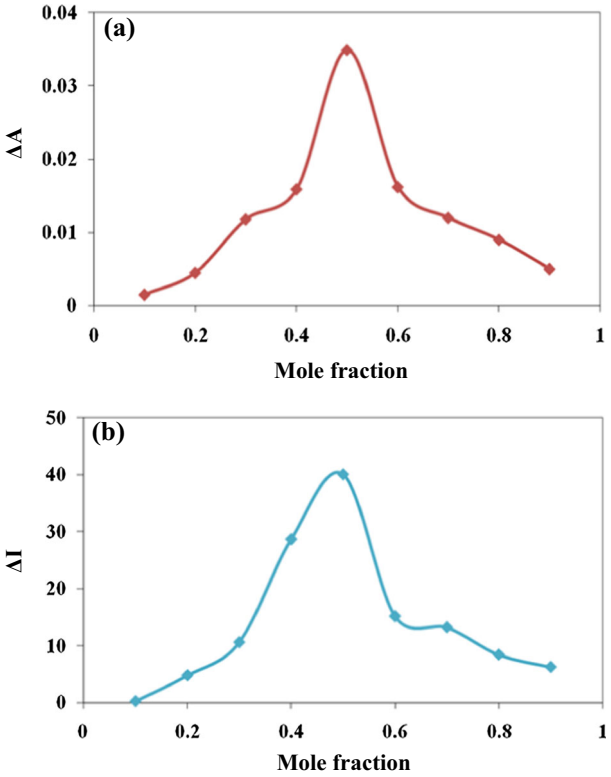

Fig. 2 **a** Job's plot ΔA versus mole fraction of DNPH with β-CD and **b** Job's plot ΔI versus mole fraction of DNPH with β-CD

correlation supporting the assumption of the 1:1, DNPH:β-CD inclusion complex. The binding constant '*K*' is evaluated as 588 M^{-1}.

The fluorescence enhancement behavior of the host–guest inclusion complex (DNPH: β-CD) is an indicative factor for using the complex for chemosensory applications. The stoichiometry of the inclusion complex of DNPH and β-CD is further confirmed by Job's continuous variation method. Figure 2 shows the change in absorbance and fluorescence against the mole fraction of DNPH. In the case of the 1:1 inclusion complex, the maximum deviation will be observed for mole

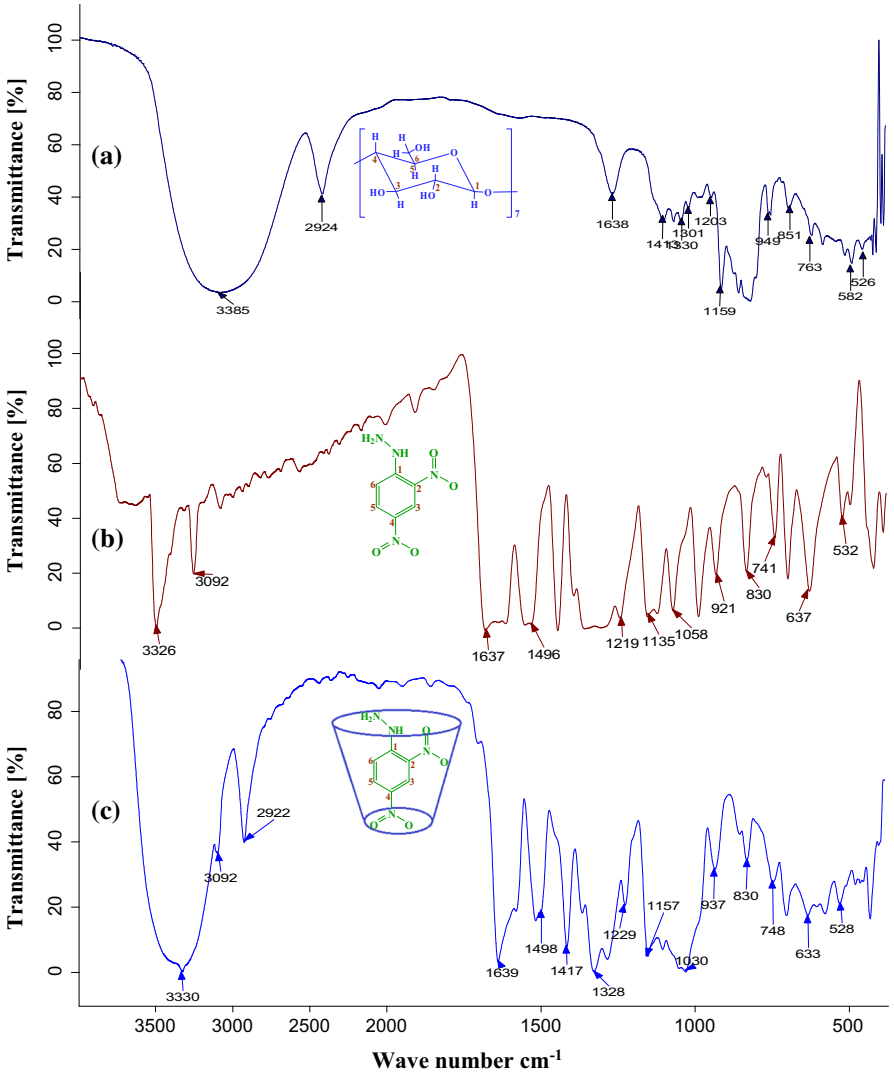

Fig. 3 FT-IR Spectra of **a** β-CD, **b** DNPH, **c** DNPH: β-CD solid inclusion complex in KBr

fraction 0.5 [69]. As shown in Job's plot, the peak maximum is obtained at mole fraction 0.5, which indicates that the inclusion complex between DNPH and β-CD has 1:1 stoichiometry.

Interaction of DNPH with β-CD in solid state

FTIR spectral analysis

There are apparent differences between the FTIR spectra of β-CD (Fig. 3a), DNPH (Fig. 3b) and DNPH: β-CD (Fig. 3c) solid inclusion complex. In the IR spectrum of DNPH (Fig. 3b) are strong peaks at 3092 cm^{-1} for the stretching vibration of C–H

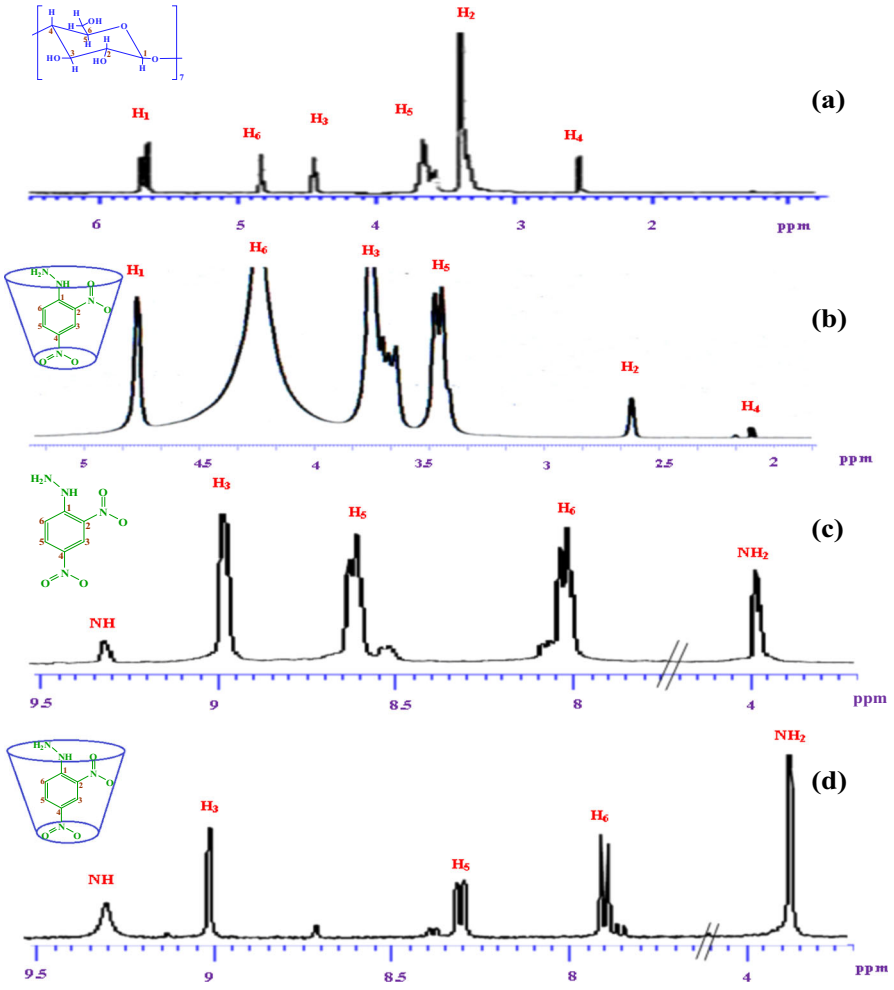

Fig. 4 H^1NMR spectra of **a** β-CD, **b** solid inclusion complex (with respect to β-CD), **c** DNPH and **d** solid inclusion complex (with respect to DNPH); determined in $CDCl_3$ at 300 K

Table 2 ^{1}H NMR chemical shifts of β-CD and β-CD:DNPH inclusion complex determined in $CDCl_3$ at 300 K

Proton	β-CD δ ppm	β-CD:DNPH inclusion complex δ ppm	$\Delta\delta$ ppm
H_1	5.697	4.995	0.702
H_2	3.374	3.348	0.026
H_3	4.460	3.575	0.885
H_4	2.513	2.590	− 0.077
H_5	3.587	3.437	0.150
H_6	4.836	3.626	1.210

Table 3 ^{1}H NMR chemical shifts of DNPH and DNPH: β-CD inclusion complex determined in $CDCl_3$ at 300 K

Proton	DNPH δ ppm	DNPH:β-CD inclusion complex δ ppm	$\Delta\delta$ ppm
H_3	7.816	7.838	− 0.022
H_5	8.408	8.321	0.087
H_6	8.764	8.761	0.003
NH	9.427	9.429	− 0.002
NH2	3.998	3.993	0.005

and 1135 cm^{-1} for the bending vibration of C–H of the aromatic ring are noted. However, in the IR spectrum of the DNPH:β-CD complex (Fig. 3c), the intensity of the peak at 3092 cm^{-1} for the stretching of C–H has been reduced due to the restriction of vibration caused by inclusion of DNPH in the β-CD nanocavity, the peak due to the bending (at 1135 cm^{-1}) vibrations of C–H has shifted to 1157 cm^{-1}. Peaks at 1637 and 1496 cm^{-1} were noted for the stretching vibration of C=C the of phenyl ring of DNPH. The stretching vibrations of C=C (at 1637 and 1496 cm^{-1}) also shifted to 1639 cm^{-1} and 1498 respectively. This is due to the presence of the phenyl ring of DNPH in the β-CD nanocavity. In the IR spectrum of DNPH, intensity of N–H stretching is very high (3326 cm^{-1}) with a sharp peak, whereas in the complex, slight shifting (to 3330 cm^{-1}) with a broader band is noted. Similarly, the peak at 1219 cm^{-1} is noted for the symmetric stretching vibration of N–O in DNPH, and it has shifted to 1229 cm^{-1} for the DNPH:β-CD complex. These are due to the limitations of vibrations in the N–H and N–O groups because of the inclusion of guest into host.

NMR spectral analysis

In Fig. 4 ^{1}H NMR spectra of β-CD, DNPH, and the β-CD:DNPH solid inclusion complex recorded in $CDCl_3$ are shown. The relevant chemical shift values are listed in Tables 2 and 3. On examining the ^{1}H NMR spectra of β-CD (Fig. 4a), β-CD:

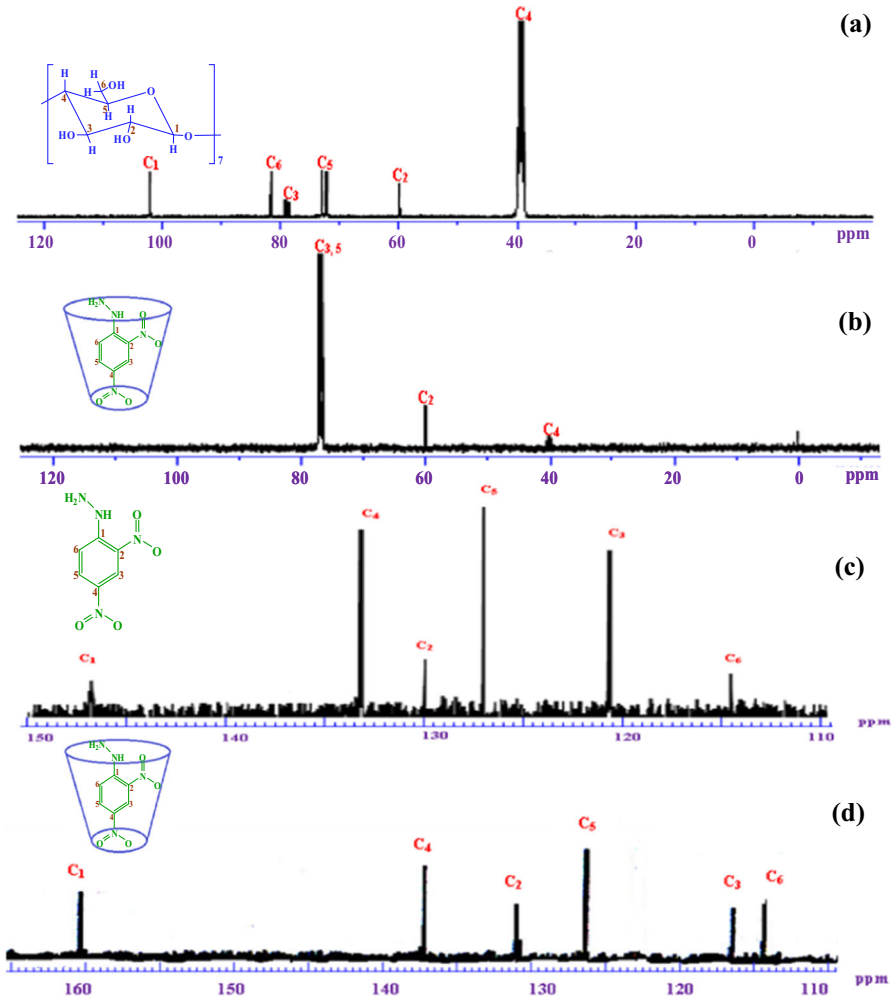

Fig. 5 ^{13}C NMR spectra of **a** β-CD, **b** solid inclusion complex (with respect to β-CD), **c** DNPH and **d** solid inclusion complex (with respect to DNPH); determined in $CDCl_3$ at 300 K

DNPH solid inclusion complex (Fig. 4b), and Table 2; significant changes in the chemical shift (δ) of H_4, H_5 and H_6 protons of β-CD are observed, and it infers the encapsulation of DNPH into the nanohydrophobic cavity of β-CD. For all the protons of β-CD, a slight shifting is observed in the chemical shifts due to the influence of the guest molecule. On examining the ^{1}H NMR spectra of DNPH (Fig. 4c), DNPH: β-CD solid inclusion complex (Fig. 4d), and Table 3; significant changes in the chemical shift (δ) of all the protons of the guest molecule (DNPH) are observed, and it infers the encapsulation of DNPH into the nanohydrophobic cavity of β-CD. In Fig. 5 ^{13}C NMR spectra of β-CD, DNPH, and β-CD:DNPH solid inclusion complex recorded in $CDCl_3$ are shown. The relevant chemical shift values are listed in Tables 4 and 5. On examining the ^{13}C NMR spectra of β-CD (Fig. 5a),

Table 4 ^{13}C NMR chemical shifts of β-CD and β-CD:DNPH inclusion complex determined in $CDCl_3$ at 300 K

Proton	β-CD δ ppm	β-CD:DNPH inclusion complex δ ppm	$\Delta\delta$ ppm
C_1	102.01	–	–
C_2	59.96	60.04	0.08
C_3	79.30	77.35	− 1.95
C_4	40.13	40.29	0.16
C_5	73.06	76.72	3.66
C_6	81.62	–	–

Table 5 ^{13}C NMR chemical shifts of DNPH and DNPH: β-CD inclusion complex determined in $CDCl_3$ at 300 K

Proton	DNPH δ ppm	DNPH:β-CD inclusion complex δ ppm	$\Delta\delta$ Ppm
C_1	145.50	161.12	− 15.62
C_2	130.11	133.46	− 3.35
C_3	121.14	119.60	1.54
C_4	133.98	139.29	− 5.31
C_5	127.28	129.04	− 1.76
C_6	115.25	117.63	− 2.38

the β-CD: DNPH solid inclusion complex (Fig. 5b), and Table 4; signals for C_1 and C_6 of β-CD disappear and, on complexation, significant changes in the chemical shift (δ) of C_2, C_3, C_4, C_5 of β-CD are observed with drastic changes in the intensity on complexation with DNPH. This is inferred due to the encapsulation of DNPH into the nanohydrophobic cavity of β-CD. Similarly, ^{13}C NMR spectra of DNPH (Fig. 5c), complex (Fig. 5d), and in Table 5; show significant changes in the chemical shift (δ) of all the carbons of the guest molecule (DNPH) as are observed, and it infers the encapsulation of DNPH into the nanohydrophobic cavity of β-CD.

Interaction of DNPH with β-CD in virtual state

Molecular docking study of the inclusion process

The molecular docking investigations performed using the PatchDock server confirm the formation of a stable docked model of DNPH: β-CD 1:1 complex (Fig. 6c) with the optimized complementarity score 2558, and energy − 214.96 kcal/mol (Table 6).

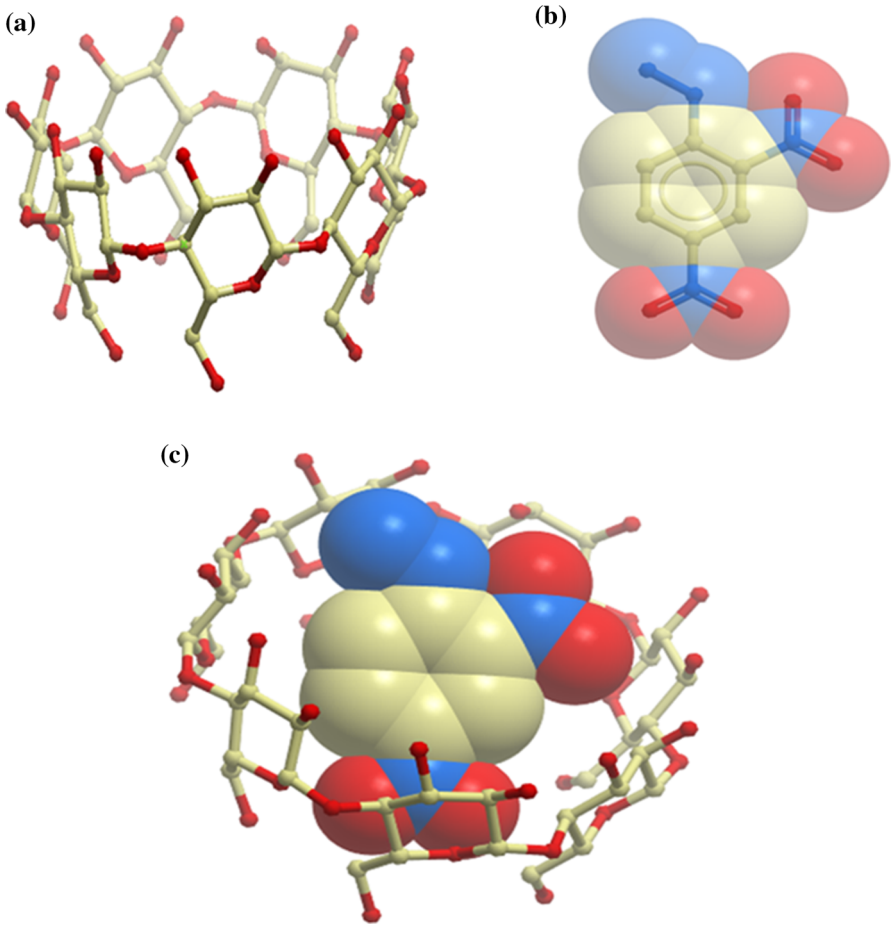

Fig. 6 Ball and stick representation of **a** β-CD, **b** DNPH, **c** 1:1 inclusion complex; the oxygen atoms are shown as red, carbon atoms are shown as golden balls and sticks, and hydrogen atoms are not shown

Semi-empirical quantum mechanical calculations

The internal diameter of the β-CD is approximately 6.5 Å and its height is 7.8 Å (Scheme 1). Considering the shape and dimensions of β-CD, it is clear that the DNPH molecule cannot be completely included in the β-CD cavity. Because, the overall height of DNPH is 8.2 Å (i.e., the vertical distance between $H_{20} - O_8$), but the overall height of β-CD is only 7.8 Å. Hence, it is possible to locate half of the DNPH molecule inside the β-CD cavity as interpreted using experimental data and as shown in Scheme 1.

Table 6 Scores of the top ten docked models of DNPH: β-CD inclusion complex computed using PatchDock server

Model	Geometric shape complementarity score	Approximate interface area size of the complex Å^2	Atomic contact energy kcal/mol
1	2558	269.10	− 214.96
2	2462	271.00	− 215.10
3	2450	257.80	− 214.88
4	2392	254.10	− 203.24
5	2374	250.30	− 195.46
6	2372	247.90	− 197.80
7	2316	267.10	− 205.13
8	2238	258.20	− 199.30
9	2202	246.20	− 191.53
10	2178	245.70	− 203.85

Orientation preference analysis

Single point energy computation for identifying the energetically favourable model

The single point energy *for Orientation 1*: orientation of hydrazine group of DNPH towards the 2° rim of β-CD (Fig. 7a), and *Orientation 2*: orientation of a nitro group containing DNPH towards the 2° rim of β-CD (Fig. 7b) are computed using AM1 and PM6 methods. The single point energy versus distance plot of *Orientation 1* and *Orientation 2* computed using AM1 and PM6 method [70] is shown in Fig. 8a, b, respectively. In the plot, the energy variation from 0 to − 6 and 0 to + 6 Å represent the variation of complexation energy for the movement of the guest molecule towards the 1° rim (narrow rim) and towards the 2° rim (wide rim) of the host molecule, respectively. For "*Orientation 1"* the energy of the complex varies in the range of − 6107.176 to 1596.3 kJ mol^{-1}. *Orientation 1* reaches the minimum energy of − 6107.176 kJ mol^{-1} at 0 Å. In the case of *Orientation 2,* the energy of the complex varies in the range of − 6457.155 to − 4956.944 kJ mol^{-1}. *Orientation 2* reaches the minimum energy of − 6457.155 kJ mol^{-1} at 0 Å. Based on the computed point energy, the most stable complex models of "*Orientation* 1" and "*Orientation* 2" are identified and energy minimization of the selected models is carried out by AM1 and the PM3 method for optimizing its geometry. The optimized model of "*Orientation* 1" is named as "complex c1" (Fig. 7c) and the complex of "*Orientation* 2" is named as "complex c2" (Fig. 7d). The energy change involved in the formation of the 1:1 DNPH:β-CD complex are calculated using the equation,

$$\Delta E = E_{(\text{DNPH: }\beta\text{–CD complex})_{\text{opt}}} - \left[E_{(\text{DNPH})_{\text{opt}}} + E_{(\beta\text{–CD})_{\text{opt}}}\right]$$

where $E_{(\text{DNPH})_{\text{opt}}}$, $E_{(\beta\text{–CD})_{\text{opt}}}$ and $E_{(\text{DNPH: }\beta\text{–CD complex})_{\text{opt}}}$ are the optimized energy values of DNPH, β-CD and the DNPH:β-CD complex, respectively. The optimized

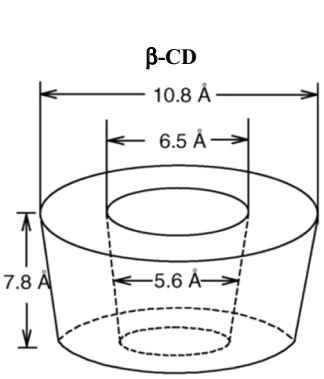

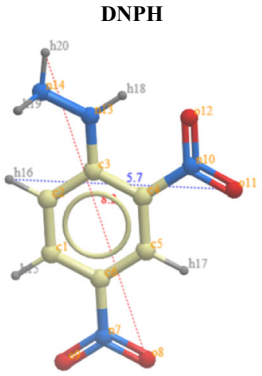

DNPH bond distance in Å		Orientation
$H_{20}-O_8$	8.2	Vertical
$H_{16}-O_{11}$	5.7	Horizontal

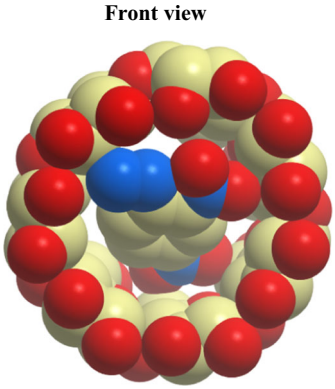

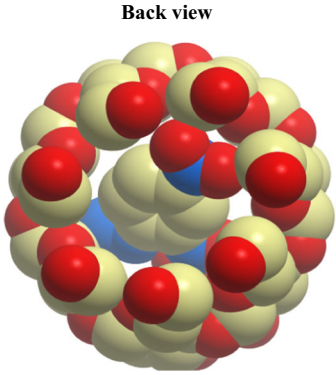

Scheme 1 DNPH: β-CD 1:1 host - guest mechanism

energy (E_{opt}) values of host, guest and two possible forms of complexes (c1 and c2), and the calculated energy change (ΔE) values are listed in Table 7. The negative complexation energies of complexes given in Table 7 infer that both the orientations can form stable inclusion complexes. From the energy (E and ΔE) values, it is evident that the complex in which the nitro group of DNPH towards the 2° rim of β-CD (i.e., complex c2) is the energetically favourable model since the ΔE for complex c2 (− 558.706 kJ mol^{-1}) is a highly negative value than is complex c1 (− 208.727 kJ mol^{-1}) with the energy difference of 349.979 kJ mol^{-1} between two complexes.

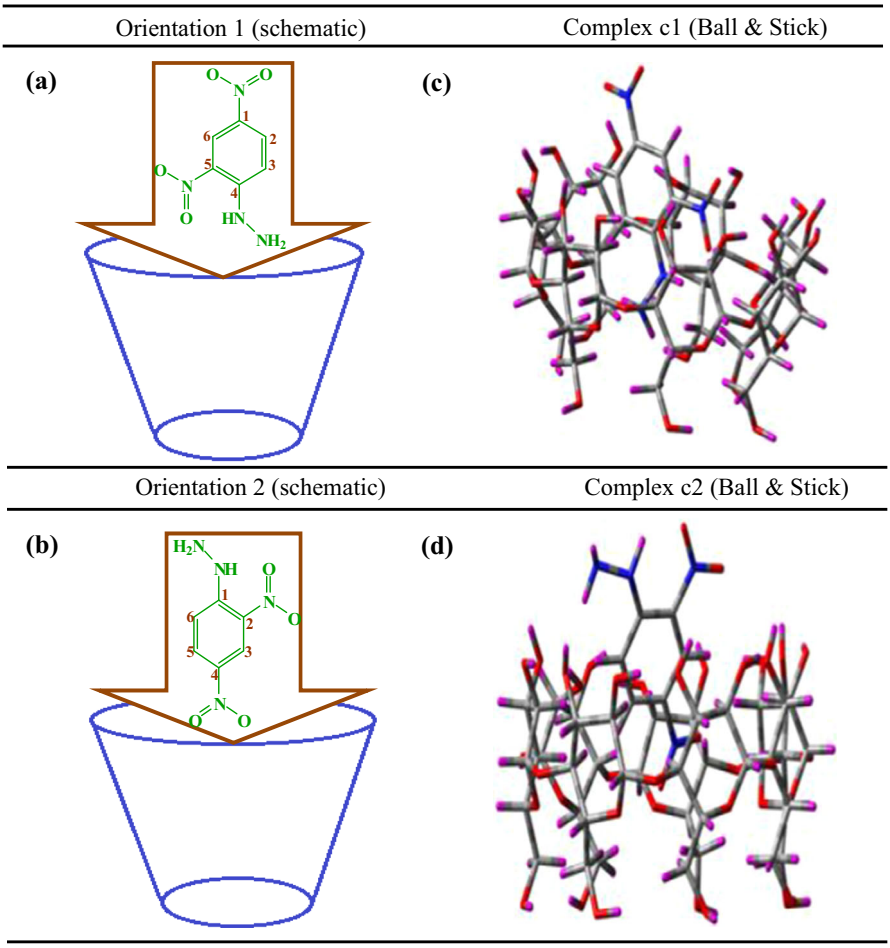

Fig. 7 DNPH:β-CD orientation preference analysis. **a** Orientation 1, **b** Orientation 2, **c** complex c1; optimized complex model of orientation 1, **d** complex c2; optimized complex model of Orientation 2

E_{HOMO}–E_{LUMO} of frontier molecular orbitals of complexes

The energy difference between the LUMO and HOMO orbitals (E_{HOMO}–E_{LUMO}) is one of the important factors in understanding the stability of the molecules. In general, inclusion complexes with larger E_{HOMO}–E_{LUMO} (i.e., energy difference between HOMO and LUMO orbital) values are highly stable; hence, the complex c2 (orientation of the nitro group containing DNPH towards the 2° rim of β-CD) is a highly favorable model since the E_{HOMO}–E_{LUMO} for complex c2 [E_{HOMO}–E_{LUMO} = 8.028 eV] is higher (Table 7 and Fig. 9) than complex c1 [E_{HOMO}–E_{LUMO} = 7.747 eV].

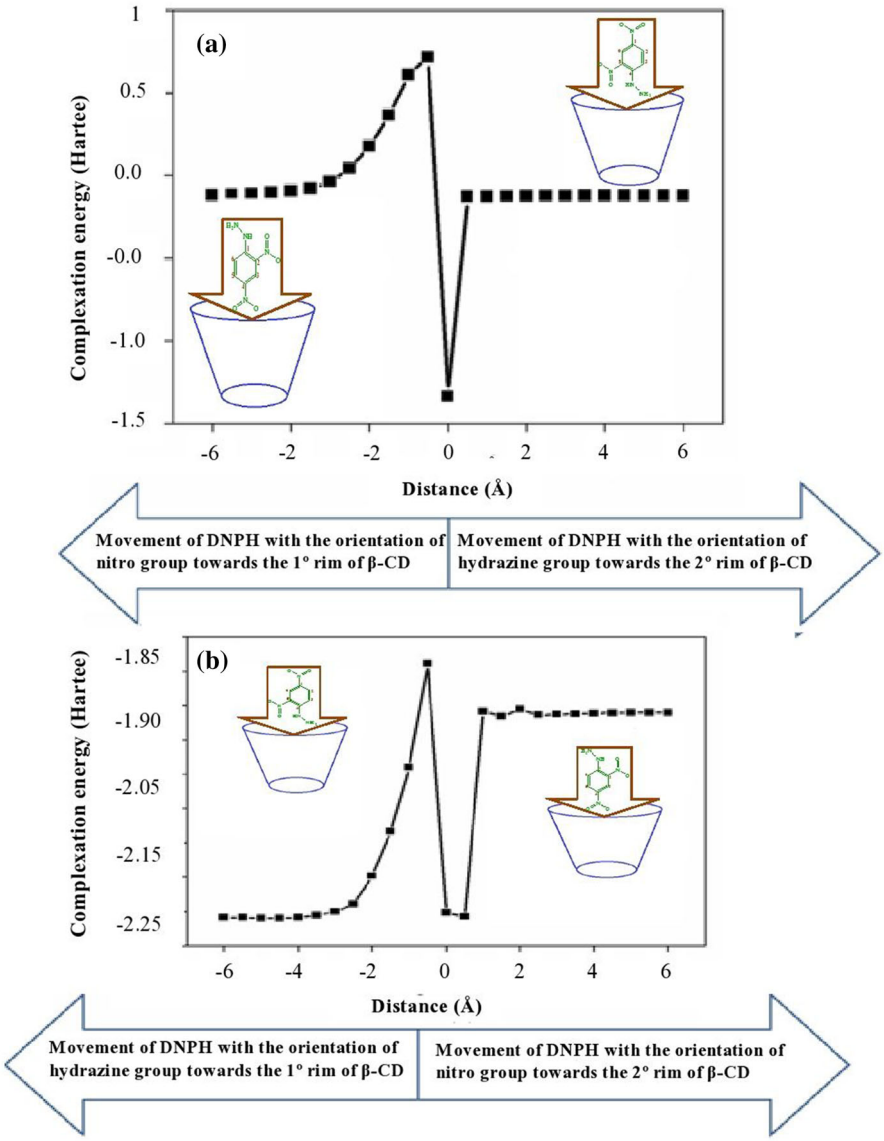

Fig. 8 Energy versus distance plot of **a** Orientation 1; **b** Orientation 2

Electrostatic potential maps of complexes

Figure 10 represents the molecular electrostatic potential (MEP) maps of complexes "c1" and "c2". Blue regions are exceptionally positive and red regions are negative neutral regions are in between yellow and green. In complex c2 significant delocalizations of electrons are observed between guest and host regions. Due to the

Table 7 Energy values of guest, host and complexes c1 and c2

Parameter	DNPH		CD		Complex C1		Complex C2	
	AM1	PM6	AM1	PM6	AM1	PM6	AM1	PM6
E_{Opt} (KJ/mol)	300.094	152.541	− 6512.851	− 6050.990	− 6669.295	− 6107.176	− 6689.774	− 6457.155
ΔE (KJ/mol)	–	–	–	–	− 454.474	− 208.727	− 477.053	− 558.706
E_{HOMO} (ev)	− 9.768	− 9.670	− 10.177	− 10.095	− 9.695	− 10.179	− 9.725	− 10.283
E_{LUMO} (ev)	− 1.790	− 1.921	0.963	− 0.360	− 1.695	− 2.432	− 1.5891	− 2.255
E_{HOMO}- E_{LUMO} (ev)	7.978	7.749	11.14	9.735	8.000	7.747	8.136	8.028

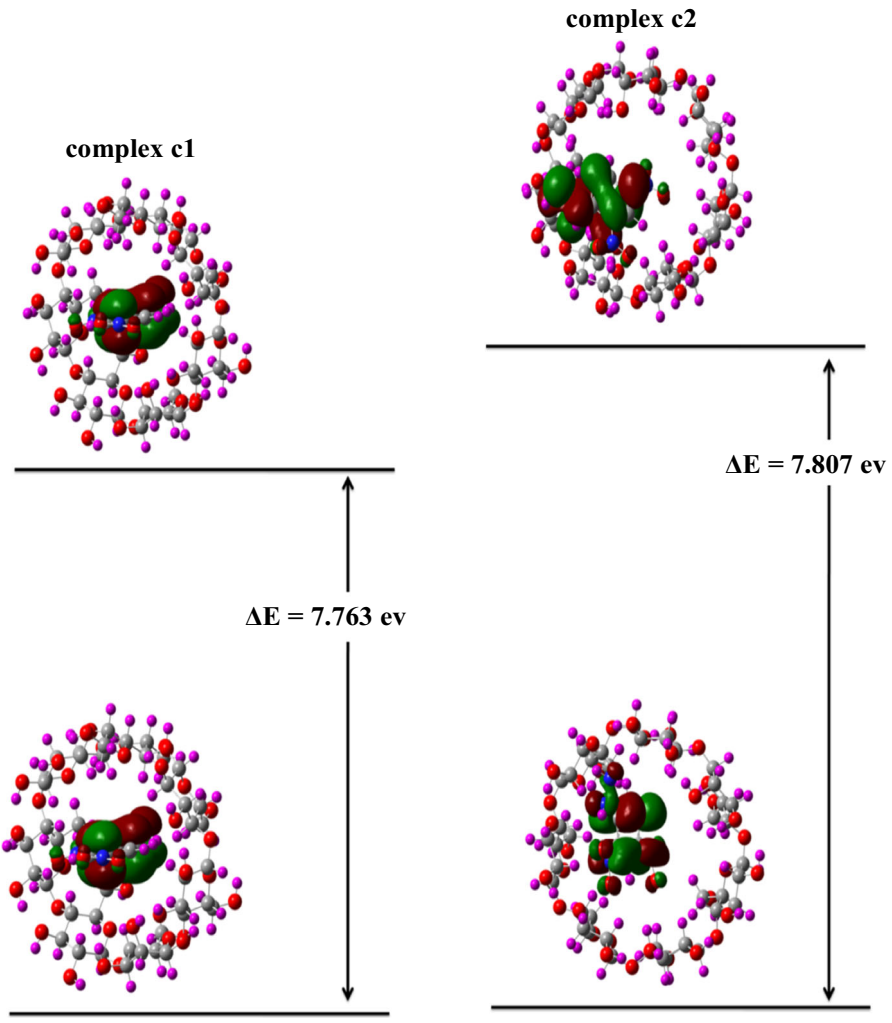

Fig. 9 HOMO-LUMO orbitals of DNPH:β-CD complex c1 and c2

delocalization of electrons, a reduced steric repulsion guest molecule has conveniently fit in the cavity of the host.

Analytical application of DNPH: β-CD complexes as chemosensors for Ce^{4+} detection

Metal sensing ability of DNPH: β-CD complex

During complex formation studies using the fluorescence technique, the DNPH: β-CD complex showed a continuous intensity enhancement which is an indicative factor for using the complex for chemosensory applications. Hence, with the aim of

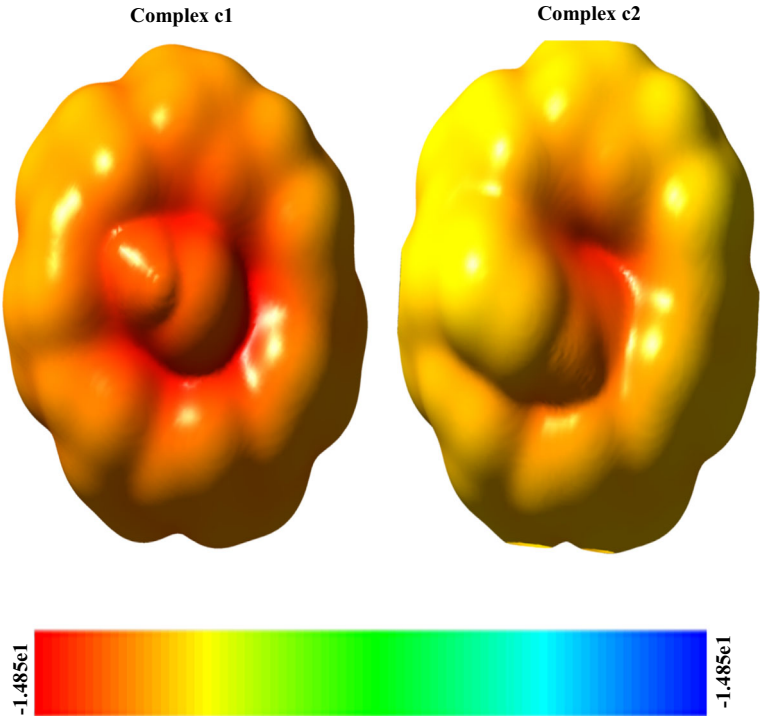

Fig. 10 Electrostatic potential maps at the van der Waals surface of DNPH:β-CD complex c1 and c2

estimating the chemical sensing abilities of the formed complex, emission spectra of a DNPH: β-CD inclusion complex in the presence of various metals were recorded to study the metal sensing behavior of the complex. Figure 11a, b shows the fluorescence spectra of DNPH: β-CD complex in the absence of metal (metal free) and in the presence of various metals such as K^{+}, Na^{+}, Hg^{2+}, Fe^{2+}, Cu^{2+}, Mn^{2+}, Co^{2+}, Mg^{2+}, Pb^{2+}, Ni^{2+}, Ca^{2+}, Ba^{2+}, Zn^{2+}, Cd^{2+}, Ag^{2+}, Al^{3+}, Fe^{3+}, Th^{4+}, Ti^{4+} Ce^{4+}. The addition of all the above metal ions to the inclusion complex did not produce any significant change, whereas the metal ion Ce^{4+} has enhanced the fluorescence intensity of the DNPH: β-CD complex significantly.

The stoichiometry of the inclusion complex of DNPH and Ce^{4+} is further confirmed by Job's continuous variation method. Figure 12 shows the change in absorbance and fluorescence against a mole fraction of DNPH. In the case of the 1:1 inclusion complex, the maximum deviation will be observed for the mole fraction 0.5 [71]. As shown in Job's plot, the peak maximum is obtained at the mole fraction 0.5, which indicates that the inclusion complex between DNPH and Ce^{4+} has 1:1 stoichiometry.

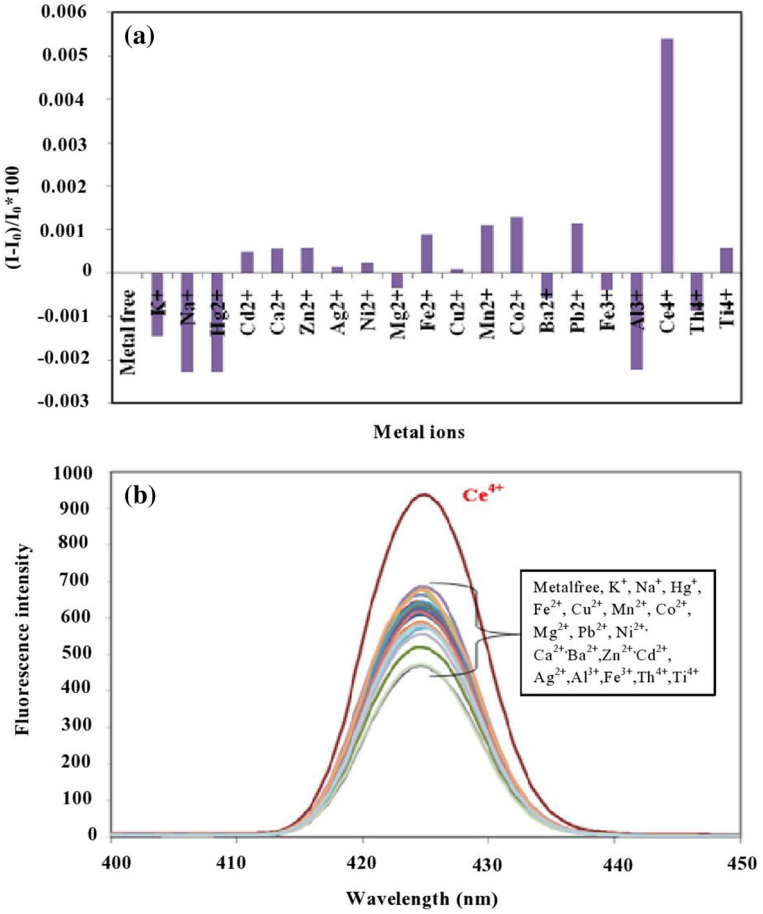

Fig. 11 **a** Fluorescence intensity change profile of DNPH: β-CD complex [concentration of DNPH: 10^{-3} M, β-CD: 12×10^{-3} M] in pH $\sim$ 7 solution the in presence of different metal cations (10^{-4} M). **b** Fluorescence spectra of DNPH: β-CD complex in the presence of different metal ions

Selectivity of DNPH: β-CD complex towards Ce^{4+}

With the aim of developing the DNPH:β-CD complex as a chemosensor for Ce^{4+} detection, fluorescence spectra of DNPH:β-CD complex + Ce^{4+} + other metal ions (K^+, Na^+, Hg^{2+}, Fe^{2+}, Cu^{2+}, Mn^{2+}, Co^{2+}, Mg^{2+}, Pb^{2+}, Ni^{2+}, Ca^{2+}, Ba^{2+}, Mn^{2+}, Zn^{2+}, Cd^{2+}, Ag^{2+}, Al^{3+}, Fe^{3+}, Th^{4+}, Ti^{4+}) were recorded. Figure 13 shows that the fluorescence intensity enhancement effect by Ce^{4+}on the chemosensor (DNPH: β-CD complex) is not influenced upon adding all other metal ions. This observation implies that the sensor has a very high degree of selectivity on Ce^{4+}. Hence, the DNPH: β-CD complex can be used as a fluorescence probe for Ce^{4+}sensing in an aqueous medium.

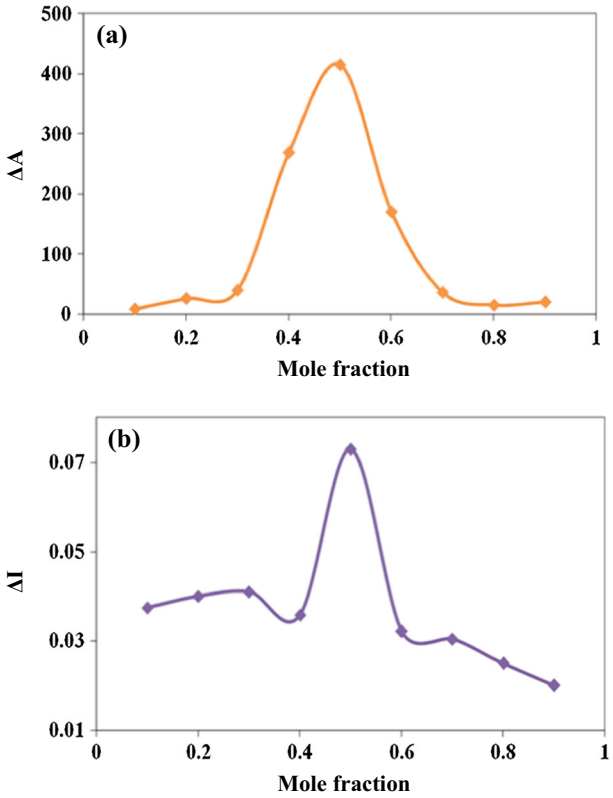

Fig. 12 **a** Job's plot ΔA versus mole fraction of DNPH: β-CD with Ce^{4+} and **b** Job's plot ΔI versus mole fraction of DNPH: β-CD with Ce^{4+}

Sensitivity of DNPH: β-CD complex towards Ce^{4+}

Fluorescence spectra of DNPH: β-CD complex + different concentrations of Ce^{4+}were recorded to estimate the sensitivity of chemosensor towards Ce^{4+}. Figure 14 shows the fluorescence spectra of chemosensor for the different concentrations of Ce^{4+} ions. The fluorescence intensity was found to be rectilinear and enhances upon increasing the concentration of Ce^{4+}ions from 0 to 10^{-15} M. This result confirms that the DNPH: β-CD complex can be used as a chemosensor for detecting Ce^{4+} ions in an aqueous medium. The analytical parameters for the sensing of Ce^{4+} using DNPH: β-CD chemosensor is shown in Table 8. The possible reaction mechanism for the fluorescence enhancement of DNPH: β-CD chemosensor with Ce^{4+} ions is proposed as shown in Scheme 2. Scheme 2 is based on the understanding that Ce^{4+} prefers to join/interact with (1) an easily accessible group of the guest, (2) group with less steric hindrance, and (3) group with a rich electron environment, in the host–guest complex. Ce^{4+} prefers to interact with the *o*-nitro group rather than the *p-nitro* group. Because, the *p-nitro* group is positioned at the 1° rim of β-CD, which is under more steric hindrance than the *o-nitro* group

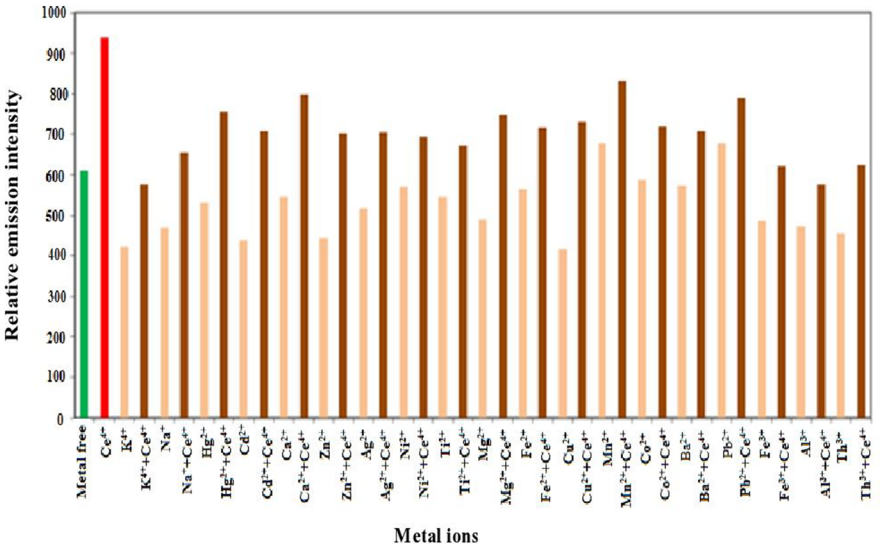

Fig. 13 Fluorescence intensity change profile of DNPH: β-CD chemosensor [concentration of DNPH: 10^{-3} M, β-CD: 12×10^{-3} M] to 10^{-4} M Ce^{4+} in the presence of other metal cations (10^{-4} M) in pH7 solution

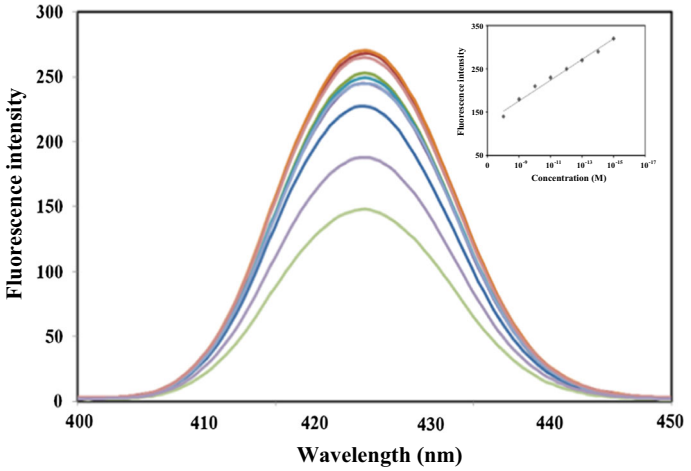

Fig. 14 Fluorescence titration spectra of DNPH: β-CD chemosensor in presence of different concentration of $Ce4^{+}$ ions. Inset: "intensity versus concentration" plot

(positioned at the 2° rim of β-CD). Ce^{4+} on complexing with the *o-nitro* group, the non-radiative energy, lost by the guest molecule in the absence of $Ce^{4+,}$ is ceased there by emission of the guest molecule that is consolidated, and; hence, fluorescence intensity enhances due to the development of the rigid fit of "guest + Ce^{4+}" inside the β-CD nanocavity.

Table 8 Experimental parameters for the sensing of Ce^{4+}using DNPH: β-CD chemosensor

λ excitation (nm)	366
λ emission (nm)	425
Linear range (M)	1×10^{-8}–1×10^{-15}
Correlation coefficient (*r*)	0.95
LOD (M)	2.9×10^{-10}
LOQ (M)	9.0×10^{-10}

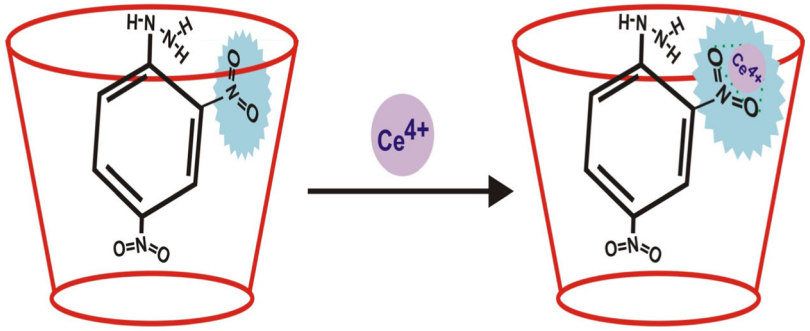

Scheme 2 Possible reaction mechanism and the proposed structure of complex formed between the DNPH: *β*-CD complex and Ce^{4+}

The results obtained for the sensing of Ce^{4+} using DNPH: β-CD complex was compared with the reports existing in the literature, and it infers that the proposed method is more effective than the methods reported earlier (Table 9). But, the reason for the fluorescence intensity enhancement of DNPH:β-CD complex with Ce^{4+} is not known clearly and it is a worthy question for further investigations. Hence, investigations on the mechanism of fluorescence enhancement/quenching due to the addition of Ce^{4+}/other metal ions on the reported chemosensor are in progress in our laboratory and will be published elsewhere.

Conclusion

Inclusion complex formation between 2,4-dinitrophenyl hydrazine and β-cyclodextrin were investigated in liquid, solid and virtual states. The binding constants of the complex were estimated using UV–visible and fluorescence spectral analysis. The solid complex was characterized and confirmed using FT-IR and NMR techniques. For orientation preference analysis, two different orientations of guest into host molecule are considered. The estimated stabilization energies, E_{HOMO}–E_{LUMO}, and MEP maps of complexes infer that the guest molecule prefers the orientation in which it experiences lesser steric repulsion effect and scores as highly stable and energetically favourable. Molecular docking and semi-empirical analysis were used

Table 9 Comparison of proposed method with the reported methods

Method	Reaction with	Linear range	LOD	Molar absorptivity ($l\ mol^{-1}cm^{-1}$)	pH	Ref.
Spectrophotometric	p-Nitroaniline	4–20 μg ml^{-1}	–	1.39×10^3	–	[55]
Spectrophotometric	Azocalixarene	5×10^{-6}–2.5×10^{-5} mol l^{-1}	2.5×10^{-6} $mol^{-1}cm^{-1}$	7.81×10^4	5–7	[56]
Spectrophotometric	Malachite green-iodide system	0.6–4.6 μg ml^{-1}	–	1.36×10^5	4.5–5.5	[57]
Spectrophotometric	Benzoic hydrazone	0.7–7.0 μg ml^{-1}	–	2.0×10^4	–	[58]
Spectrofluorimetric	2, 6-Diamino toluene	1–40 gml^{-1}	–	4.04×10^3	–	[59]
Spectrofluorimetric	Ascorbic acid	0.0531 μg ml^{-1}	0.0145 μg ml^{-1}	–	3.4	[60]
Kinetic-Potentiometric	$K_2Cr_2O_7$	1–30 μg ml^{-1}	0.45 μg ml^{-1}	–	3	[62]
Spectrofluorimetric	DNPH-Bcd	1×10^{-8}–1×10^{-15} mol l^{-1}	2.9×10^{-10} mol l^{-1}	1.64×10^2	7	This work

as a supporting evidence for the results observed from the experimental analysis. The chemosensing behavior of DNPH: β-CD complex was carried out using fluorescence spectroscopy. The estimated LOD: 2.9×10^{-10} and LOQ: 9.0×10^{-10}. This result suggests that the solid state sensor based on the DNPH: β-CD complex could be a promising sensory material for developing a sensory device for detecting Ce^{4+}.

References

1. C.F. Allen, Org. Synth. Coll. **2**, 228 (1943)
2. V. Chis, S. Filip, V. Miclaus, V. Pirnau, A. Pirnau, M. Vasilescu, J. Mol. Struct. **744**, 363 (2005)
3. M. Kosalec, S. Bakmaz, S. Pepeljnjak, S. Vladimir Knezevic, Acta Pharm. **54**, 65 (2004)
4. S. Gupta, R.C. Husser, R.S. Geske, S.E. Welty, C. Smith, Toxicol. Sci. **54**, 203 (2000)
5. D. Udhayakumaria, S. Velmathia, Y.-M. Sungb, S.P. Wub, Sens. Actuators, B **198**, 285 (2014)
6. S.S. Kanolkar, V.T. Walke, Int. J. Pharm. Pharm. Sci. **6**, 0975 (2014)
7. K. Sowjanya, J.C. Thejaswini, B.M. Gurupadayya, M.I. Priya, Der Pharmacia Lettre. **3**, 47 (2011)
8. E.G. Anthon, M.D. Barrett, J. Sci. Food Agric. **83**, 1210 (2003)
9. J. Dhrubajyoti Majumdar, Chem. Cheml. Sci. **5**, 749 (2015)
10. S.M. Siddagangappa, S.M. Mayanna, F. Pushpanadan, Anti. Corros. Method M. **23**, 11 (1976)
11. Y.-L. Lin, P.-Y. Wang, L.-L. Hsieh, K.H. Ku, Y.T. Yeh, C.H. Wu, J. Chromatogr. A **1216**, 6377 (2009)
12. E. Floor, M.G. Wetzel, J. Neurochem. **70**, 268 (1998)
13. F. Lipari, S. Swarin, Environ. Sci. Technol. **19**, 70 (1985)
14. S. Jitjaicham, P. Kampalanonwat, P. Supaphol, Express Polym. Lett. **10**, 832 (2013)
15. J. Szejtli, Chem. Rev. **98**, 1743 (1998)
16. M.V. Rekharsky, Y. Inoue, Chem. Rev. **98**, 1875 (1998)
17. T. Loftsson, M.E. Brewster, J. Pharm. Sci. **101**, 3019 (2012)
18. F. Hapiot, S. Tilloy, E. Monflier, Chem. Rev. **106**, 767 (2006)
19. P. Brocos, N. Diaz-Vergara, X. Banquy, S. Perez-Casas, M. Costas, A. Pineiro, J. Phys. Chem. B. **39**, 12455 (2010)
20. T. Kristmundsdottir, T. Loftsson, W.P. Holbrook, Int. J. Pharm. **139**, 63 (1996)
21. H. Kublik, T.K. Bock, H. Schreier, B.W. Muller, Eur. J. Pharm. Biopharm. **42**, 320 (1996)
22. T. Loftsson, E. Stefansson, Drug Dev. Ind. Pharm. **23**, 473 (1997)
23. H. Dome, Eur. J. Pharm. Biopharm. **39**, 133 (1993)
24. P. Jarho, A. Urtti, D.W. Pate, P. Suhonen, T. Jarvinen, Int. J. Pharm. **137**, 209 (1996)
25. E. Fenyvesi, M. Vikmon, L. Szente, Crit. Rev. Food Sci. Nutr. **56**, 1981 (2016)
26. J. Wang, Y. Cao, B. Sun, C. Wang, Food Chem. **127**, 1680 (2011)
27. G. Astray, C.G. Barreiro, J.C. Mejuto, R.R. Otero, J. Simal Gandara Food Hydrocoll. **23**, 1631 (2009)
28. V.A. Marcolino, G.M. Zanin, L.R. Durrant, M.D. Benassi, G. Matioli, J. Agric. Food Chem. **59**, 3348 (2011)
29. L. Bardi, A. Mattei, S. Steffan, M. Marzona, Enzyme Microb. Technol. **27**, 709 (2000)
30. D. Arockia Jency, M. Umadevi, G.V. Sathe, J. Raman Spectrosc. **46**, 377 (2015)
31. B.J. Reid, K.T. Jhones, PCT Int Appl **54**, 727 (1999)
32. A.R. Hedges, Chem. Rev. **98**, 2035 (1998)
33. J. Sumaoka, W. Chen, Y. Kitamura, T. Tomita, J. Yoshida, M. Komiyama, J. Alloys Compd. **408**, 391 (2006)
34. I.D. Nickson, C. Boxall, A. Jackson, G.O.H. Whillock, I.O.P. Conf, Ser. Mater. Sci. **9**, 1 (2010)
35. H.J. Vieira, O. Fatibello, Quim. Nova **28**, 797 (2005)
36. W.W. Monafo, S.N. Tandon, V.H. Ayvazian, J. Tuchschmidt, A.M. Skinner, F. Deitz, Surgery **80**, 465 (1976)
37. W.-X. Tang, P.-X. Gao, MRS Commun. **63**, 11 (2016)
38. T. Yamaguchi, N. Ikeda, H. Hattori, K. Tanabe, J. Catal. **67**, 324 (1981)

39. V.D. Kosynki, A.A. Arzgatkina, E.N. Ivanov, M.G. Chtoutsa, A.I. Grabk, A.V. Kardapolov, N.A. Sysina, J. Alloys Compd. **303**, 421 (2000)
40. M. Melchionna, P. Fornasiero, Mater. Today **17**, 349 (2014)
41. A.N. Shmyreva, A.V. Borisov, N.V. Maksimchuk, Nanotechnol. Russ. **5**, 5 (2010)
42. J.K. Kar, R. Stevens, C.R. Bowen, Adv. Appl. Ceram. **106**, 175 (2007)
43. K. Otsuka, M. Hatano, A. Morikawa, J. Catal. **79**, 493 (1983)
44. B. Gantt, S. Hoque, R.D. Willis, K.M. Fahey, J.M. Delgado-Saborit, R.M. Harrison, G.B. Erdakos, P.V. Bhave, K.M. Zhang, K. Kovalcik, H.O.T. Pye, Environ. Sci. Technol. **48**, 10607 (2014)
45. S. Sendilvelan, K. Bhaskar, S. Nallusamy, Rasayan j. chem. **10**, 454 (2017)
46. M.S. Hirst, S.A. Karakoti, D.R. Tyler, N. Sriranganathan, S. Seal, M.C. Reilly, Small **24**, 2848 (2009)
47. A. Gojova, J.-T. Lee, H.S. Jung, B. Guo, A.I. Barakat, I.M. Kennedy, Inhal Toxicol. **21**, 123 (2009)
48. S. Mittal, A.K. Pandey, BioMed Res. Int. **1** (2014)
49. A. Arya, A. Gangwar, S.K. Singh, M. Roy, M. Das, N.K. Sethy, K. Bhargava, Int. J. Nanomedicine. **11**, 1159 (2016)
50. H.E. Liying, S.U. Yumin, J. Lanhong, S.H.I. Shikao, J. Rare Earths **33**, 791 (2015)
51. D. Bouzid, N. Belkhie, T. Aliouane, Mater. Sci. Eng. **28**, 1 (2012)
52. J.-H. Maeng, S.-C. Choi, J. Opt Soc Korea. **16**, 414 (2012)
53. A. Nemmar, S. Al-Salam, S. Beegam, P. Yuvaraju, B.H. Ali, Int. J. Nanomedicine. **12**, 2913 (2017)
54. S.K. Nalabotu, M.B. Kolli, W.E. Triest, J.Y. Ma, N.D. Manne, A. Katta, H.S. Addagarla, K.M. Rice, E.R. Blough, Int. J. Nanomedicine. **6**, 2327 (2011)
55. C.V. Bhaskar, B. Shyla, G. Nagendrappa, Asian J. Biochem. Pharma Res. **1**, 2231 (2011)
56. L. Van Tan, N. Thi Ngoc Le, Int. J. Chem. Eng. Appl. **2**, 6 (2011)
57. K. Etesh Janghel, Y. Pervez, J. Sci. Ind. Res. **68**, 940 (2009)
58. C.K. Rao, V.K. Reddy, T.S. Reddy, Talanta **41**, 237 (1994)
59. S. Jihad, A. Al Shaheen, College of Basic Education Researchers Journal. **8**, 4 (2009)
60. M.M. Karim, S.H. Lee, Y.S. Kim, H.S. Bae, S.B. Hong, J. Fluoresc. **16**, 1 (2006)
61. M.A. Karimi, M.H. Mashhadizadeh, M. Mazloum-Ardakani, F. Rahavian, Am. J. Anal Chem. **2**, 73 (2010)
62. D. Schneidman-Duhovny, Y. Inbar, R. Nussinov, H.J. Wolfson, Nucl. Acids Res. **33**, 363 (2005)
63. M.L. Connolly, Science **221**, 709 (1983)
64. M.L. Connolly, J. Appl. Crystallogr. **16**, 548 (1983)
65. C. Zhang, G. Vasmatzis, J.L. Cornette, C. DeLisi, J. Mol. Biol. **267**, 707 (1997)
66. M.J. Frisch,, G.W. Trucks, H.B. Schlegel,, G.E. Scuseria,, M.A. Robb, J.R. Cheeseman, J.A. Montgomery Jr., T. Vreven, K.N. Kudin, J.C. Burant, J.M. Millam, S.S. Iyengar, J. Tomasi, V. Barone, B. Mennucci, M. Cossi, G. Scalmani, N. Rega, G.A. Petersson, H. Nakatsuji, M. Hada, M. Ehara, K. Toyota, R. Fukuda, J. Hasegawa, M. Ishida, T. Nakajima, Y. Honda, O. Kitao, H. Nakai, M. Klene, X. Li, J.E. Knox, H.P. Ratchian, J.B. Cross, C. Adamo, J. Jaramillo, R. Gomperts, R.E. Stratmann, O. Yazyev, A.J. Austin, R. Cammi, C. Pomelli, J.W. Ochterski, P.Y. Ayala, K. Morokuma, G.A. Voth, P. Salvador, J.J. Dannenberg, V.G. Zakrzewski, S. Dapprich, A.D. Daniels, M.C. Strain, O. Farkas, D.K. Malick, A.D. Rabuck, K. Raghavachari, J.B. Foresman, J.V. Ortiz, Q. Cui, A.G. Baboul, S. Clifford, J. Cioslowski, B.B. Stefanov, G. Liu, A. Liashenko, P. Piskorz, I. Komaromi, R.L. Martin, D.J. Fox, T. Keith, M.A. Al-Laham, C.Y. Peng, A. Nanayakkara, M. Challacombe, P.M.W. Gill, B. Johnson, W. Chen, M.W. Wong, C. Gonzalez, J.A. Pople, Gaussian 03, Revision A.1, Gaussian, Inc., Pittsburgh PA (2003)
67. P. Job, Annali di Chimica Applicata. **9**, 113 (1928)
68. H.A. Benesi, J.H. Hildebrand, J. Am. Chem. Soc. **71**, 2703 (1949)
69. X. Ge, J. He, Y. Yang, F. Qi, Z. Huang, L. Ruihua, L. Huang, X. Yao, J. Mol. Struct. **994**, 163 (2011)
70. D. Duhovny, R. Nussinov, H.J. Wolfson, in Proceedings of the 2'nd Workshop on Algorithms in Bioinformatics(WABI), Rome, Italy, Lecture Notes in Computer Science, ed. by Gusfield et al. vol. 2452 (Springer, Berlin, 2002), p. 185
71. K. Sivakumar, M. Nichodemus, K.R. Sankaran, Mol. Phys. **112**, 1879 (2014)